ACTA
AMAZONICA | http://dx.doi.org/10.1590/1809-4392201804681

ORIGINAL ARTICLE

Provenance of heavy and clay minerals in bottom sediments of Green Lake, an Amazonian fluvial lake in Brazil

Anderson C. MENDES[1]*, Ângela B. DANTAS[2], Anne Caroline S. RIBEIRO[2], Livaldo O. SANTOS[2], Kamilla C. MENDES[3], Dorsan dos Santos MORAES[1], Rodolfo M. ALMEIDA[2]

[1] Universidade Federal do Pará - UFPA, Instituto de Geociências, Campus Guamá, Rua Augusto Correa, 01 - Guamá, 66075-110 Belém, Pará, Brazil

[2] Universidade Federal do Oeste do Pará - UFOPA, Instituto de Engenharia e Geociências, Unidade Tapajós. Rua Vera Paz s/n, Salé, 68035-110 Santarém, Pará, Brazil

[3] Universidade Federal do Oeste do Pará - UFOPA, Programa de Pós-Graduação em Sociedade, Ambiente e Qualidade de Vida, Unidade Amazônia, Av. Mendonça Furtado 2946, Fátima, 68040-470 Santarém, Pará, Brazil

* Corresponding author: acmendes@ufpa.br; https://orcid.org/0000-0002-6205-6486

ABSTRACT

Studies on provenance of minerals in Amazonian rivers focus mostly on suspended sediments, while processes that control bottom-sediment production and distribution are still little known. We determined the provenance of the bottom sediments of Green Lake, a micro-basin draining into the Tapajós River, in the eastern Brazilian Amazon. We used X-ray powder diffraction (XRD), Fourier-transform infrared spectroscopy (FTIR), scanning electron microscope (SEM) and, cathodoluminescence techniques to analyze clay, light and heavy minerals of 22 samples. The lake is L-shaped, with 5.5 m maximum depth, and predominance of mud over sand in the center. Quartz and feldspar were dominant in the light fraction, while zircon, tourmaline, kyanite, rutile, and staurolite were dominant in the heavy fraction. The clay fraction was dominated by kaolinite, with morphology and degree of crystallinity indicative of a detrital origin related to weathering. The Alter do Chão Formation (ACF) is suggested as the main source of sand sediments and heavy minerals, due to their mineralogical and percentage similarity. The provenance of kaolinite was mainly the ACF, with a minor contribution of the Amazon and Tapajós rivers. The primary origin of the heavy minerals in the ACF indicates the basement of the Amazonas Basin as source rock and this formation as a source of sediments for Green Lake through weathering and erosion processes under current tropical conditions. The presence of *Aulacoseira granulata* and *Aulacoseira ambigua* indicates the importance of current erosive processes on sediment production.

KEYWORDS: Alter do Chão Formation, lacustrine sediment, Amazon Basin, Santarém, mineral characterization

Proveniência de minerais pesados e argilominerais em sedimentos de fundo do Lago Verde, um lago fluvial amazônico no Brasil

RESUMO

Estudos de proveniência em rios amazônicos concentram-se principalmente em sedimentos suspensos, enquanto os processos que controlam a produção e distribuição de sedimentos de fundo ainda são pouco conhecidos. Sedimentos de fundo do Lago Verde foram estudados com o objetivo principal de determinar a proveniência sedimentar. Utilizamos técnicas de difração de raios-X em pó (DRX), espectroscopia no infravermelho com transformação de Fourier (FTIR), microscopia eletrônica de varredura (MEV) e catodoluminescência para analisar argilas e minerais pesados em 22 amostras. O Lago Verde tem forma em L, profundidade máxima de 5.5 m, com predomínio da fração lama sobre areia no centro do lago. Quartzo e feldspato foram dominantes na fração leve, e zircão, turmalina, cianita, rutilo e estaurolita na fração pesada. A fração argila foi dominada por caulinita, cuja morfologia e grau de cristalinidade indicam origem detrítica relacionada com ação intempérica. A Formação Alter do Chão (FAC), substrato do Lago Verde, é indicada como principal fonte dos sedimentos arenosos e minerais pesados, dada a semelhança mineralógica e percentual. A caulinita foi derivada da FAC, mas não como única fonte. Os rios Amazonas e Tapajós têm uma pequena contribuição para a proveniência da caulinita. A origem primária dos minerais pesados na FAC indica o embasamento da Bacia do Amazonas como rochas fonte, e esta formação funciona com fonte de sedimentos para o Lago Verde, a partir dos processos de intemperismo e erosão, sob condições tropicais atuais. A presença de *Aulacoseira granulata* e *Aulacoseira ambigua* indicou o papel importante dos processos erosivos atuais na produção de sedimentos.

PALAVRAS-CHAVE: Formação Alter do Chão, sedimentos lacustres, Bacia Amazônica, Santarém, caracterização mineral

CITE AS: Mendes, A.C.; Dantas, Â.B.; Ribeiro, A.C.S.; Santos, L.O.; MENDES, K.C.; Moraes, D.S.; Almeida, R.M. 2020. Provenance of heavy and clay minerals in bottom sediments of Green Lake, an Amazonian fluvial lake in Brazil. *Acta Amazonica* 50: 159-169.

INTRODUCTION

Amazonian rivers drain regions with different reliefs and erosion rates (Wittmann *et al.* 2010), as well as several types of rocks from Cambrian to Cenozoic ages (Coutinho 2008). The Tapajós and the Xingu river basins have approximately 500,000 km^2 and are the main clear-water tributaries of the Amazon River, with a low sedimentation rate compared to other Amazonian rivers (Latrubesse *et al.* 2005).

The Tapajós Basin has an elevation gradient from 800 m in the headwater region to 7 m downstream (ANA 2011). It originates at the confluence of the Juruena and Teles Pires rivers and extends for 800 km until it discharges into the Amazon River (Figure 1). It drains crystalline and sedimentary rocks from the Central Brazilian Shield, which is characterized by relatively low sediment concentration and slightly alkaline waters (Sioli 2011). Along its path, several tributaries encounter the Tapajós River, forming micro-basins.

The Green Lake (*Lago Verde*, in its local denomination) is a micro-basin that drains into the Tapajós River close to its mouth on its right bank and is strongly influenced by variations in the level of the Tapajós River, which has an annual average flow rate range of 4,000 to 30,000 m^{3}s^{-1}, while that of the Amazon River varies from 105,000 to 235,000 m^{3}s^{-1} (ANA 2018). Due to its higher flow rate, the Amazonas River acts as a hydraulic barrier at the mouth of the Tapajós, preventing the entrance of a great part of the suspended and bottom sediments from the Tapajós into the Amazon (Sorribas *et al.* 2016).

In Green Lake, this hydraulic barrier becomes "drowned" during the four-month period of higher rainfall (February to May) in the two catchments (Amazon and Tapajós), which favors water accumulation and internal sedimentation (Nascimento *et al.* 1976). The hydraulic barrier is a widespread geomorphological phenomenon throughout the Amazonas Basin (Nascimento *et al.* 1976; Cohen *et al.* 2014; Park and Latrubesse 2015; Gualtieri *et al.* 2017), yet little is known regarding the distribution of sediments which varies widely along the Tapajós River due to erosive and sedimentological processes (Medeiros Filho *et al.* 2016). These processes are influenced by many factors, such as rock and soil types, vegetation cover, margin slope, topographic compartments, and rainfall regime (Carvalho 2008).

Sedimentological studies in Amazonian fluvial systems have focused on the origin and transport of suspended load sediments (e.g. Guyot *et al.* 2007; Viers *et al.* 2008), dissolved solids (e.g. Moquet *et al.* 2016), physicochemical aspects (e.g. Sousa *et al.* 2009), heavy metals (e.g. Nevado *et al.* 2010), and carbon in sediments (e.g. Bertassoli Jr. *et al.* 2017). However, little is known about the sources and the transport of sand as bed loads or its relationship with suspended sediments in Amazonian rivers (Sawakuchi *et al.* 2018). The characteristics of the sediments can be used to interpret changes in a river system (Wampler 2012), and to understand the factors that control sediment production, transport, and accumulation (Lord *et al.* 2009). The characteristics and origin of the bottom sediments of the Green Lake remain unknown.

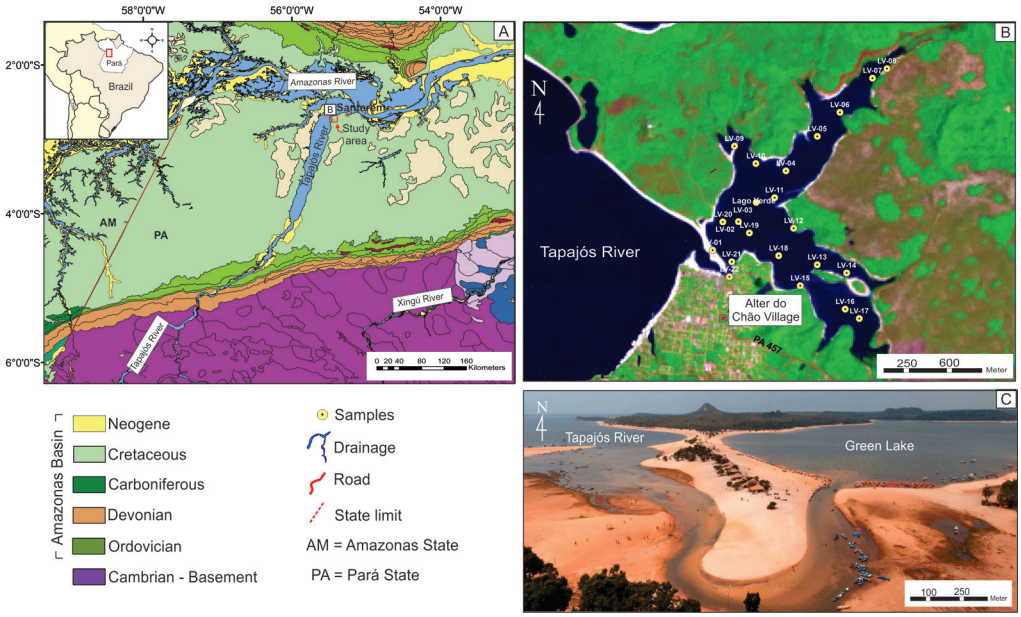

Figure 1. A – Geological context of the Tapajós River drainage in the western region of Pará state (northern Brazil) showing the location of Green Lake; B – Map of Green Lake showing the distribution of the sampling points; C – Photograph of the Green Lake and the Tapajós River separated by a sand bar. This figure is in color in the electronic version.

Considering the hydrological characteristics of the Green Lake, the lack of information on its sedimentology and the relation between sandy and muddy sediments, we aimed to identify, characterize and determine the provenance of the bottom sediments of the lake, and their relationship with the dynamics of the Tapajós and Amazon rivers. We focused on clay minerals, due to their wide applicability in the geosciences, to evaluate the maturity of suspended sediments, weathering intensity, and to identify areas that are sources of contemporary rocks, fluvial sediments, and marine sediments (Zuther *et al*. 2000; Suresh *et al.* 2004).

MATERIAL AND METHODS

Geological and regional settings

In Brazil, the Amazonas Basin drains Cenozoic sediments and sedimentary rocks from river plains. The Tapajós River drains a large area of the Amazonian Craton with exposed Precambrian rocks (Sawakuchi *et al*. 2018), however, most of its sediment sources are related to the sedimentary rocks from the Amazonas Basin, represented by Paleozoic and Cretaceous rocks, recent deposits and complex river bars (Figure 1).

Green Lake is located on the Alter do Chão Formation, which is formed by red sandstone, argillites, conglomerates, and intraformational breccias attributed to high-energy river systems (Daemon 1975) and fluvio-lacustrine-deltaic systems (Mendes *et al*. 2012; Mendes 2015). The climate in the region is hot and humid (Am type in the Köppen classification), and the vegetation is ombrophilous dense forest, with a few areas of open ombrophilous forest, Cerrado savanna (at the mouth Tapajós River mouth), and floodplain forests along the river margins, with a terrain characterized by a morphoclimatic domain in dissected plateaus and pediplains (Nascimento *et al*. 1976; Rocha 2014).

Sampling and analyses

To determine the provenance of sediments, a planimetric map was created to indicate the spatial distribution of the samples, using multispectral images with spatial resolution Landsat 8, OLI sensor, WGS 84 and UTM Zone 23 (Figure 1b). Twenty-two samples (0.5 kg each) of bottom sediment were collected using a Van Veen Grab sampler and we sought to cover the entire lake area. A bathymetric map was created to determine the depth of the lake and observe its relationship to the distribution of sediments. The depth measurements were taken with graded rulers at each sample collection point. We screened and centrifuged 15 g of each sample to define the mud and sand proportion, and to create sediment-distribution maps of each fraction. The bathymetric and sediment maps were analyzed with geostatistical methods, using ordinary kriging with semivariogram fitting and interpolation.

For the analytical analysis, the sediments were divided into clay-sized and sand-sized fractions. The sand-sized fraction was then subdivided into light and heavy minerals. The clay and sand fractions were analyzed with X-ray diffraction (XRD) at the Geosciences Institute of Universidade Federal do Pará (UFPA) with the following conditions: 2° to 70° 2θ 40kV and 40mA for powder analysis, and 2° to 40° 2θ for clay mineral analysis.

To identify light minerals 5 g of sample was pressed pellets and used for the powder method. Three steps were used to identify the clay minerals: air drying, ethylene glycol saturation, and heating at 550 °C for two hours. The XRD data were interpreted through the X'Pert HighScore Plus Panalytical software. The degree of crystallinity of the kaolinite was determined through the Amigó Index (Amigó *et al.* 1987). Fourier-transform infrared (FTIR) spectrums of the clay minerals were obtained in the infrared region by attenuated total reflectance (ATR) with a Thermo Scientific Nicolet iS50 FT-IR Spectrometer utilized in the 4000-400 cm^{-1} region. The samples were pulverized, then dried at 105 °C for 24 hours. Data were acquired through the OMNIC software.

To estimate the proportion of light minerals, 100 grains were counted per sample under a Zeiss binocular stereomicroscope. The heavy minerals were extracted from the very fine- to fine-sized sand with bromoform (2.89 g cm^{-3}). The heavy minerals were identified, characterized and quantified based on the count of at least 200 grains per sample under a Zeiss petrographic microscope. Mineralogical maturity was determined by the ZTR index (Hubert 1962).

Scanning electron microscopy (SEM) images were obtained to characterize the morphology of clay minerals, the surface textures of heavy minerals and identification of diagnostic diatom species of the genus *Aulacoseira* Thwaites. Cathodoluminescence-SEM images were used for the internal structures of zircon. These images were obtained at the SEM Laboratory of UFPA with a LEO1450VP SEM microscope.

RESULTS

The Green Lake is L-shaped, oriented in NE-SW and NW-SE direction. We measured a maximum depth of 5.5 m at the center of the lake (Table 1; Figure 2a). Despite its extension, the extrapolation of depth measurements indicated that the lake is relatively flat and shallow (Figure 2a).

The samples were constituted of mud-sized and fine- to coarse-sand grains. The sand fraction accumulated mainly in the marginal portions of the lake, reaching nearly 100% at some points, and grain size tended to increase towards the margins (Table 1a; Figure 2b). The mud fraction occurred in all samples and prevailed in the central portion of the lake, where it reached up to 98% (Figure 2c).

Light minerals had similar mineralogy in all samples, with quartz dominance (Figure 3). Quartz grains were hyaline, white and matte, with angular and subangular forms prevailing over sub-rounded forms. We observed feldspar, rutile, zircon and opaque minerals. The amount of quartz ranged from 78.4

Table 1. Location, depth and characterization of grain size, heavy mineral proportion and kaolinite cristalinity in 22 samples of bottom sediments collected in Green Lake (Tapajós River basin, Pará state, Brazil). Sample codes refer to the spatial distribution in Figure 1b.

Sample	UTM coordinates		Depth (m)	Grain size (%)[a]		Heavy minerals in sand fraction (%)[b]										Kaolinite cristalinity[c]	
	X	Y		Sand	Mud	Zir	Tou	Rut	kya	Sta	Ana	Sil	Gar	Spi	ZTR	FWHM (001)	FWHM (002)
LV 01	727526	9723610	0.5	98.6	1.4	83.5	6.0	2.0	1.5	4.0	1.0	2.0	0.0	0.0	91.5	0.414	0.353
LV 02*	727861	9723964	4.8	2.3	97.7	---	---	---	---	---	---	---	---	---	---	0.453	0.340
LV 03	728207	9724356	4.8	2.3	97.7	86.5	4.7	2.0	2.0	2.8	1.0	1.0	0.0	0.0	93.2	0.315	0.300
LV 04	728673	9724850	1.8	99.8	0.2	90.2	3.2	1.3	1.8	2.2	0.0	0.9	0.4	0.0	94.7	0.341	0.301
LV 05	729165	9725390	1.8	99.3	0.7	87.3	5.9	1.0	1.0	3.0	0.8	1.0	0.0	0.0	94.2	0.408	0.320
LV 06	729519	9725765	2.0	7.1	92.9	83.5	7.0	1.5	2.0	3.0	1.0	1.5	0.0	0.5	92.0	0.369	0.352
LV 07	730030	9726300	1.0	56.0	44.0	84.8	6.1	1.5	3.0	3.0	0.3	1.0	0.3	0.0	92.4	0.434	0.339
LV 08	730256	9726449	1.0	36.8	63.2	83.5	7.5	2.0	2.5	3.5	0.0	1.0	0.0	0.0	93.0	0.411	0.361
LV 09	727867	9725236	0.5	15.9	84.1	87.2	4.4	0.5	2.9	3.0	0.5	1.0	0.0	0.5	92.1	0.435	0.368
LV 10	728203	9724964	2.5	9.7	90.3	88.0	4.0	1.0	2.5	3.5	0.0	1.0	0.0	0.0	93.0	0.416	0.335
LV 11	728497	9724430	3.0	38.1	61.9	86.5	4.0	1.0	2.5	4.0	0.5	1.5	0.0	0.0	91.5	0.374	0.329
LV 12	728794	9723951	0.5	99.3	0.7	88.8	7.1	0.9	1.7	0.5	0.0	0.5	0.0	0.5	96.8	0.422	0.325
LV 13	729164	9723381	3.5	11.5	88.5	83.8	7.6	1.5	2.3	1.9	1.0	1.9	0.0	0.0	92.9	0.411	0.313
LV 14	729625	9723252	2.5	18.5	81.5	82.0	10.5	1.0	2.5	2.0	0.5	1.5	0.0	0.0	93.5	0.418	0.358
LV 15	728897	9723053	2.5	93.4	6.6	90.2	6.3	0.5	1.5	1.0	0.0	0.5	0.0	0.0	97.0	0.419	0.338
LV 16	729602	9722686	2.5	8.0	92.0	83.0	9.5	1.0	2.0	1.5	1.5	1.5	0.0	0.0	93.5	0.411	0.329
LV 17	729823	9722539	0.5	99.8	0.2	68.1	22.2	0.5	1.8	6.4	0.0	0.5	0.0	0.5	90.8	0.447	0.334
LV 18	728560	9723522	4.8	3.0	97.0	79.0	12.0	1.5	3.0	3.5	0.0	1.0	0.0	0.0	92.5	0.394	0.331
LV 19	728101	9723878	5.5	4.4	95.5	77.5	13.0	0.5	2.5	5.0	0.0	1.5	0.0	0.0	91.0	0.377	0.346
LV 20	727685	9724051	3.5	99.9	0.1	79.0	12.5	1.0	2.0	5.0	0.0	0.5	0.0	0.0	92.5	0.358	0.327
LV 21	727825	9723428	0.5	99.9	0.1	77.5	15.0	1.0	1.0	5.0	0.0	0.5	0.0	0.0	93.5	0.401	0.339
LV 22	727789	9723192	0.15	99.9	0.1	89.1	4.2	3.2	1.0	1.5	0.0	1.0	0.0	0.0	96.5	0.410	0.345

a Proportion of sand and clay fraction;
b Proportion of transparent and non-micaceous heavy minerals in the sand-sized fraction (0.062 – 0.0125 mm). Zir = zircon; Tou = tourmaline; Rut = rutile; Kya = kyanite; Sta = staurolite; Ana = anatase; Sil = sillimanite; Gar = garnet; Spi = spinel; ZTR = zircon + tourmaline + rutile index; --- = data absent.
c Crystallinity degree of kaolinite from Green Lake calculated from FWHM (001) and FWHM (002).
*Heavy mineral analysis not done.

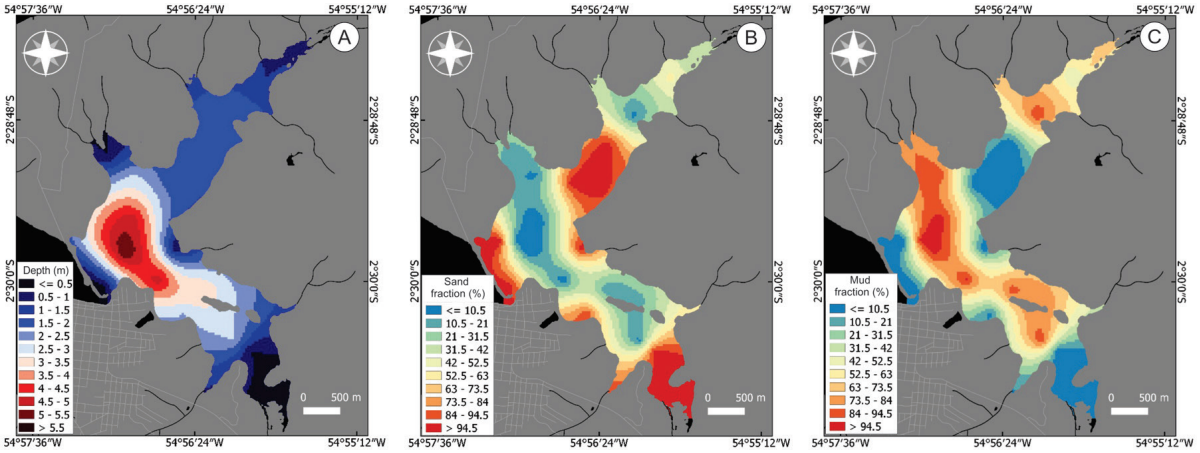

Figure 2. Maps of Green Lake (Tapajós River basin, Pará state, Brazil) showing the distribution of depth (A); sand fraction (B); and mud fraction (C), obtained through semivariogram fitting, and ordinary kriging interpolation based on 22 bottom-sediment samples. This figure is in color in the electronic version.

to 98%, followed by feldspars, with up to 24.1%, while all others did not exceed 10%. The heavy mineral composition varied little among samples. The assemblage was formed by zircon, tourmaline, kyanite, rutile, staurolite, anatase, sillimanite, garnet and spinel (Table 1b; Figure 4).

Zircon grains were the most abundant in the assemblage, ranging from 68.1 to 90.2%. Prismatic and bipyramidal forms with slightly eroded edges, inclusions, and internal zoning were common, in addition to colorless and slightly brown grains, which were equidimensional rounded to subangular.

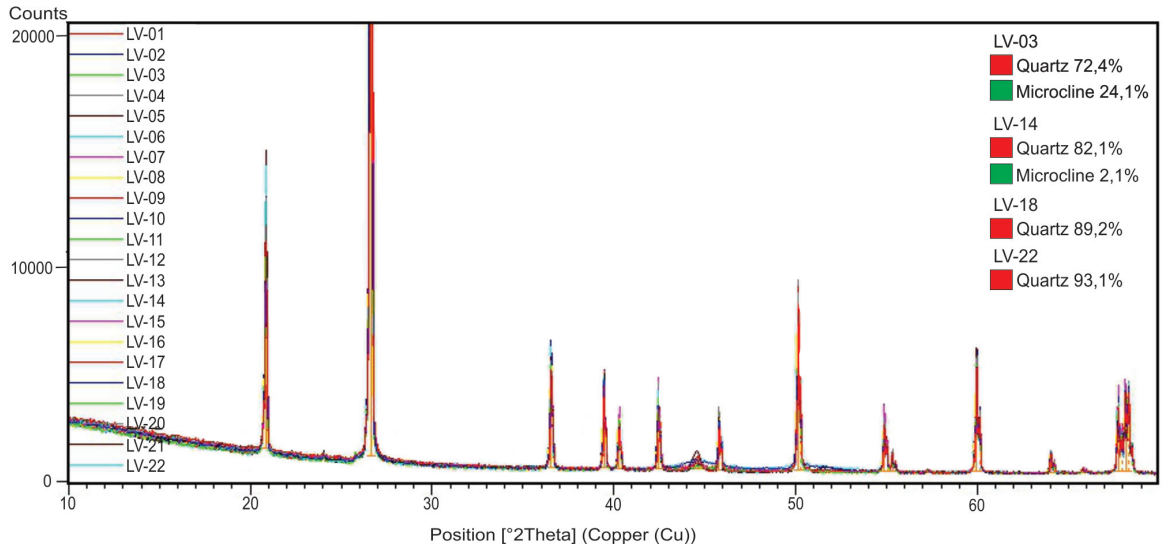

Figure 3. Sand fraction diffractogram showing some of the main minerals identified in bottom sediments of Green Lake (Tapajós River basin, Pará state, Brazil). This figure is in color in the electronic version.

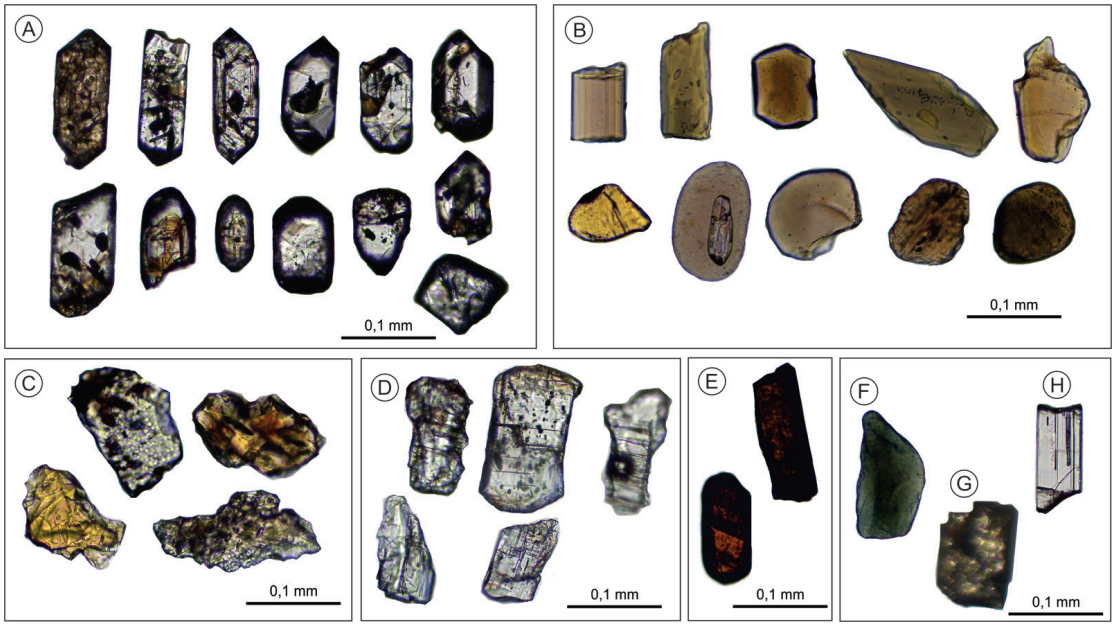

Figure 4. Photomicrographs of heavy minerals from bottom sediments of Green Lake (Tapajós River basin, Pará state, Brazil). A – zircon; B – tourmaline; C – staurolite; D – kyanite; E – rutile; F – spinel; G – anatase; H – sillimanite. This figure is in color in the electronic version.

Fractures, percussion marks, and upturned plates occurred on the surface of the grains (Figure 5a-c). Internally, some of these grains were metamitic (Figure 5d) and had concentric zoning (Figure 5e). Tourmaline composed from 3.2 to 22.2% of the samples, and exhibited green and dark-brown prismatic shapes, as well as more abundant subangular to round greenish-brown grains. Impact marks and conchoidal fractures were common (Figure 5f,g). Kyanite ranged from 1 to 3% and had prismatic and irregular shapes, with impact marks, conchoidal fractures, and spear-tip or rhombohedral shape (Figure 5i). Rutile ranged from 0.5 to 3.2%, and had irregular form, red color, sub-rounded shape and predominance of impact marks and striation lines (Figure 5j). Staurolite ranged from 0.5 to 5% and had angular grains and superficial impact marks (Figure 5h). Sillimanite ranged from 0.5 to 2%, with colorless and usually prismatic forms. The remaining heavy minerals did not occur in all samples. Anatase grains reached up to 1.5%, and had cubic shape with bluish and colorless tones. Garnet and spinel occurred in lower than 0.5% abundances. The ZTR index was above 90% in all samples.

All clay samples contained kaolinite (Figure 6a), and had a degree of crystallinity between 0.315 [FWHM (001)] and

0.300 [FWHM (002)] (Table 1c). The pattern in the infrared spectrum was similar in all samples, showing low variation in the deformation and vibration bands (Figure 6c). The bands at 3695, 3667 and 3650 cm^{-1} are related to the surface hydroxyls and the band at 3619 cm^{-1} to the internal hydroxyls (Frost 1998; Shoval *et al.* 1999; Zhu *et al.* 2016). Between 1031 and 990 cm^{-1}, the vibration bands represent the Si-O bond; at 910 cm^{-1}, the Al-OH deformation band; at 795, 751 and 52-530 cm^{-1}, the the Si-O-Al bond; and at 693-680 and 45-462 cm^{-1}, the Si-O bond (Bhaskar *et al.* 2010). The broadband presented at 1637-1632 cm^{-1} corresponds to the O-H bond of free water. Regarding the crystalline structure of kaolinite, the samples closer to the lake center had superficial and internal hydroxyls better preserved than those on the border

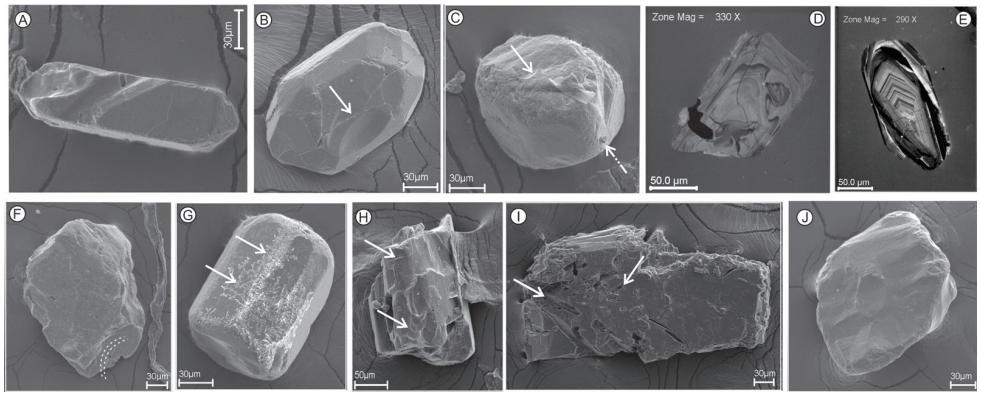

Figure 5. Scanning electron microscopy and cathodoluminescence images of the heavy mineral grains from bottom sediments of Green Lake (Tapajós River basin, Pará state, Brazil). A-C – Secondary electron imaging of zircon; D-E – metamitic and concentric zoning cathodoluminescence images of zircon grains; F – Tourmaline image with impact marks (white lines); G – Tourmaline grains with chemical dissolution (arrows); H – Staurolite with percussion marks (arrows); I – Tabular kyanite form and chemical corrosion (arrows); J – Rutile grain with transportation mark.

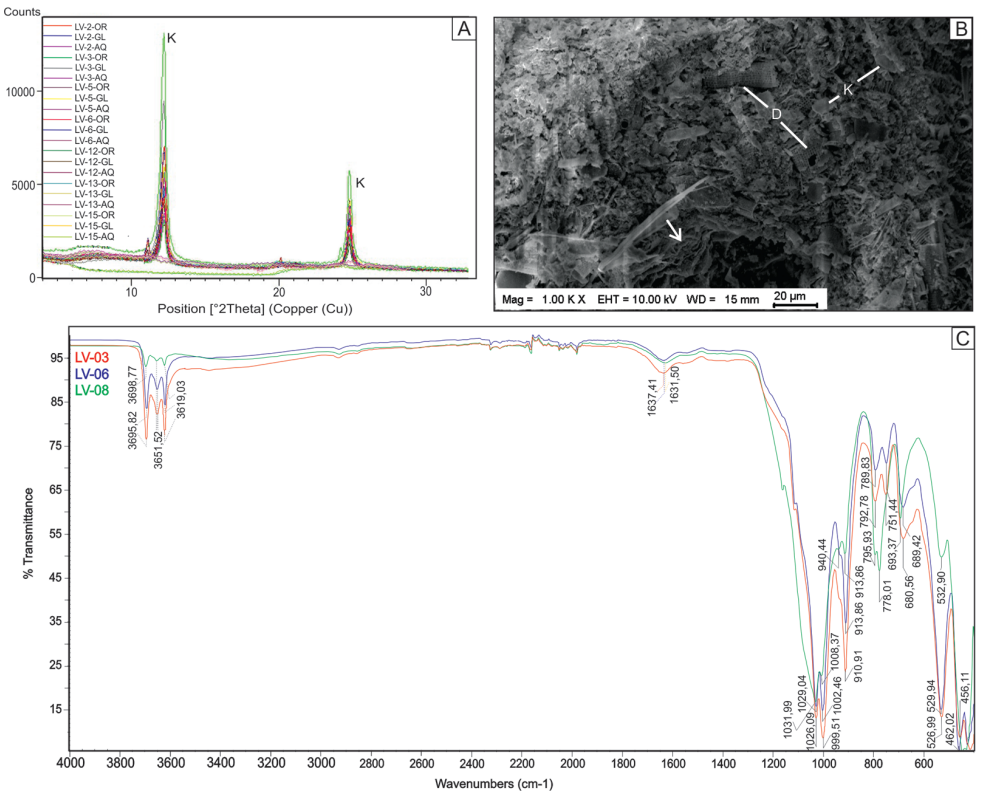

Figure 6. Group of clay minerals identified in bottom sediments of Green Lake (Tapajós River basin, Pará state, Brazil). A – Clay fraction diffractograms indicating kaolinite (K); B – SEM micrographs of a detrital kaolinite platy grain with rounded edges (K) and pseudo-booklets of kaolinite (arrow). Note the diatom groups (D) coexisting with detrital kaolinite; C – Comparison between the FTIR of kaolinite between 400 and 4000 cm^{-1} showing the characteristic stretching region of this mineral between 3550 and 3750 cm^{-1}. Note the appearance of the Al-O-Si band at 778 cm^{-1} in the sample LV-08 plus the edge of the lake. This figure is in color in the electronic version.

of the lake. Two diatom species were observed in the bottom sediments, *Aulacoseira granulata* (Ehrenberg) Simonsen 1979 and *Aulacoseira ambigua* (Grunow) Simonsen (Figure 6b).

DISCUSSION

The L-shape of the lake and the orientation of the two arms in NW/SE and NE/SW direction, at almost 90°, suggests a tectonic control similar to other Amazonian lakes (Rossetti 2014). The granulometric distribution in Green Lake, with mud in the central bottom area, increasing to coarse-sized sand on the edges, was also observed in other Amazonian lakes (Souza-Filho *et al.* 2016). Along the right bank of the Tapajós River, close to Green Lake, sand sediments predominate only from 42 m depth downwards (Irion *et al.* 2006). Thus, the large amount of sand in the Green Lake is intriguing.

The variation in proportion of quartz, microcline and other minerals in our samples was not related to the variation in sediment grain size, but to its spatial distribution. Quartz was predominant on the lake border while the proportion of other minerals increased towards the center. The predominance of angular and subangular over sub-rounded shapes in the quartz and feldspar grains can indicate short transport or proximity to the source area (Jesus *et al.* 2014; Araújo *et al.* 2015).

Quartz and feldspar are common in a wide variety of rocks. In sedimentary rocks, such as quartz-arenites, arkose and subarkose, they commonly occur as the main phases, while other minerals occur as accessory phases (Pettijohn *et al.* 1987). Green Lake is surrounded by quartz-arenites and subarkoses with regular quartz grains derived from granite, metamorphic rocks, or both (Mendes *et al.* 2013). If only igneous sources are considered, quartz grain percentages are less dependent on grain size in granite-sourced sands because of its high mechanical and chemical stability. These percentages increase with decreasing grain size in sands derived from metamorphic rocks (Tortosa *et al*. 1991). However, as the amount of quartz observed in the bottom sediments of Green Lake was not homogeneous, a mix of igneous and sedimentary sources should be assumed.

The Tapajós River drains the cretaceous cover and the rocks from the Amazonian Craton, and, due to its geological configuration, denudation rates in the Amazonian Craton are low and allow for a higher period of weathering, which causes the reduction of feldspar input in the rivers (Sawakuchi *et al.* 2018). Nevertheless, there may exist large quantities of feldspar available in the Tapajós River that serve as sources of this mineral for Green Lake.

The morphological characteristics of the heavy minerals in our samples suggest a sediment mixture and a distinctive sedimentary history and, therefore, different provenance, which would argue against a common provenance attributed to euhedral and round grains in the same sample (Krynine 1946). Surface textures of quartz grains can be used for provenance and paleoenvironmental reconstruction (Machado *et al*. 2016) and, to infer heavy mineral provenance (Moral-Cardona *et al.* 2005; Achab *et al.* 2007). The combination of surface textures observed in our samples suggests the multi-cyclical nature of the sediments. In addition, striation lines and upturned plates indicate that grains were subjected to prolonged stages of exposure to aeolian environments, while impact marks and conchoidal fractures indicate subaqueous transportation (Krinsley and Doornkamp 2011).

The mechanical superficial features observed in the ZTR grains were acquired during transport and/or deposition to the bottom of the lake, specially due to friction between grains (Krinsley and Doornkamp 2011). Among these features, the most important are the V-shaped grooves (Helland *et al.* 1997) and the conchoidal fractures, which indicate transport in a high-energy environment (Woronko *et al.* 2015). The etch pits, specially dissolution in the kyanite and staurolite grains, are related to processes of diagenesis or weathering of grains exposed for long periods (Kurumathoor and Franz 2018). The rounded to sub-rounded form and predominant superficial textures of the heavy mineral grains in our samples indicate exposure to aeolian environments (Marcinkowski and Mycielska-Dowgiałło 2013; Rajganapathi *et al.* 2013), suggesting that wind had (and may still have) an important role in the transportation of the sediments to Green Lake.

The small shapes and low diversity of colors of tourmaline grains suggest a low variety of source rocks, metamorphic and granitic rocks being the main sources of tourmaline (Mange and Maurer 2012). Zircon, like tourmaline, crystallizes in igneous rocks, and its morphology is controlled by crystallization speed, magma composition, and temperature (Corfu *et al.* 2003; Gagnevin *et al.* 2010). Zircon varieties are classified according to the shape (Sturm 2010; Shahbazi *et al.* 2014). The zircon grains from Green Lake varied widely in shape, however, shape loss due to constant mechanical abrasion renders the use of the typology ineffective in morphological studies in sedimentology (Corfu *et al.* 2003).

The oscillatory zonings observed in the zircon grains are generated during their crystallization and are not affected by superficial geological processes (Gagnevin *et al.* 2010). Only subsequent metamorphic events can alter the zoning structure, making them convoluted or homogeneous, as observed in some grains (see Figure 5d), pointing to a metamorphic source (Corfu *et al.* 2003). However, most zircon grains were euhedral (as in Figure 5a), with concentric oscillatory zoning (as in Figure 5e), indicating a primary igneous source (Gagnevin *et al.* 2010).

Kyanite, staurolite and rutile, which were found in significant amounts in our samples, are indicative of metamorphic rock contribution, as these minerals are representative of metamorphic events of medium to high degree, and are found in mica schists, schists, and, with a low frequency, in gneisses (Mange and Maurer 2012; Deer *et al.* 2013). Sillimanite also

indicates metamorphic sources, as it is found in gneisses, granulites and mica schists (Mange and Maurer 2012; Deer *et al.* 2013). The euhedral anatase grains in our samples indicate authigenic origin (Deer *et al.* 2013). During the diagenetic process, they grow and depend on the availability of titanium, which, in turn, originates from opaque mineral destabilization (Azevedo 2017). Garnet can have various sources, usually of metamorphic origin (Deer *et al.* 2013). It can also be of magmatic origin, commonly occurring in peraluminous granites (Lackey *et al.* 2012; Doucet *et al.* 2013). Garnet is relatively stable under alkaline conditions, but can have low stability in fluids with pH < 7 (Morton 1985; Andò *et al.* 2012), as is the case in Green Lake, explaining the low occurrence of this mineral. It has to be considered that the determination of the primary origin of heavy mineral grains in Green Lake is hampered by the influence of weathering conditions, that can significantly modify the mineralogical composition of rocks and sediments, eliminating the less stable minerals (Morton and Hallsworth 1994, 1999; Andò *et al.* 2012).

If the Tapajós River is the source of the heavy minerals in the bottom sediments of Green Lake, the sedimentological dynamics within the lake would be controlled by the river. However, the hydraulic-barrier effect hinders sediment transportation into the lake in the area where the Tapajós River flows into the Amazon River (Nascimento *et al.* 1976). The Amazon River is also unlikely to be the sole source for the lake sediments, as the heavy minerals in this part of the Amazonas have a very different composition (Landim *et al.* 1983; Nascimento Jr. *et al.* 2015).

Although the composition of the bottom sediments of Green Lake indicates multiple source areas for the provenance of the heavy minerals, the occurrence of a single clay mineral group suggests a single source area for the clay fraction. The origin of the kaolinite may be detrital or authigenic. Kaolinite of authigenic origin should have a delicate morphology, with an undisturbed booklet-form or vermicular structure indicative of short-distance or no transport (Chamley 1989; Moore and Reynolds Jr. 1997). When the origin of the kaolinite is detrital, it should mostly present irregular shapes and a degree of crystallinity with values of FWHM (001) and FWHM (002) always higher than 0.3 (Amigó *et al.* 1987), as was the case in our samples.

The infrared spectrum of the samples confirmed the kaolinite structure (Chukanov 2014; Zhu *et al.* 2016), which becomes disordered towards the edges of the lake due to disruption of the hydroxyl. This disruption can be related to weathering due to exposure of sediments on the edges of the lake during the low-water season. The presence of the Al-O-Si band in the samples from the lake edge corresponds to the distortions of the tetrahedral and octahedral layers, and corroborates the cation changes and disorder around the hydroxyls (Saikia and Parthasarathy 2010).

The occurrence of *Aulacoseira granulata* and *Aulacoseira ambigua* in the bottom sediments of Green Lake had already been reported by Dantas *et al.* (2017). The presence of *A. granulata* is associated with erosion and thermal variation in nutrient-rich waters (Bicudo *et al.* 2016), suggesting that erosion plays a key role in the generation of sediments for the lake. Further studies are necessary on the identification and classification of diatoms for a better understanding of their origin and their role in sediment dynamics in Green Lake.

The Alter do Chão Formation (ACF) is of siliciclastic nature and the weathering intensity causes the hydrolysis of feldspars in telogenetic conditions, leading to kaolinite neoformation (Mendes 2010; Mendes *et al.* 2013). This is a common reaction in hot and humid conditions (Brown *et al.* 2008). The mineral assemblage of the Green Lake sediments was very similar to that observed in the ACF, both in species and in percentage composition (Mendes 2010; Mendes *et al.* 2013; Mendes 2015), and the same was true for the ZTR index, which indicates ultra-stability, as expected in quartz-arenites (Pettijohn *et al.* 1987).

The presence of euhedral and sub-rounded and rounded grains in our samples indicates that almost all the sandy sediments of Green Lake are derived from the ACF, as the sediments that compose its rocks are also of multicyclic origin (Figure 4). However, only part of the kaolinite in our samples can be attributed to this formation, since it is not possible to infer the completion of the feldspar hydrolysis process, as the ACF rocks have a limited amount of feldspar (up to 20%), and are mainly constituted by quartz-arenites and subarkoses (Mendes 2010; Mendes *et al.* 2013). An alternative kaolinite source could be the Tapajós and Amazon rivers (Figure 7), as illite, chlorite, smectite, and kaolinite have been identified in sediment samples from these rivers (Guyot *et al.* 2007).

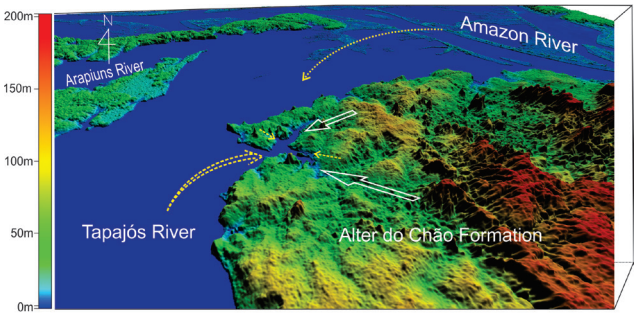

Figure 7. Digital elevation model (DEM) of the confluence of the Tapajós and Amazonas rivers, in Pará state (northern Brazil), showing the location of Green Lake (at the confluence of the arrows) and the Arapiuns River. Arrows represent the sandy sediment source areas for Green Lake from the Alter do Chão Formation (white arrows), main sources of kaolinite (double yellow broken-line arrow) and secondary sources (simple yellow broken-line arrow) from the Alter do Chão Formation and Amazonas River. DEM created from SRTM data with a spatial resolution of 30 m. Source: Earth explore, USGS. No scale. This figure is in color in the electronic version.

CONCLUSIONS

Our analyses of the bottom sediments of Green Lake, a fluvial- lake at the confluence of the Tapajós and Amazon rivers indicated that the sand sediments originated mainly from the Alter do Chão Formation (ACF). The clay minerals derived in part from ACF rock weathering, but may also originate from the Tapajós and Amazon rivers, due to the easy transportation of suspended clay sediments into the lake. The heavy mineral assemblage was formed by stable to ultra-stable minerals with a high ZTR index, and was in accordance with the relatively low feldspar content in ACF rocks, which are suggested as the origin of the heavy minerals in the lake sediments. That indicates that weathering processes were decisive in the assemblage control. The mineral assemblages were similar in species and percentage composition to those recorded in the ACF, which is likely the main source of bottom sediments in the lake. Metamorphic and igneous rocks and first-cycle sedimentary rocks were likely the primary sources of the heavy mineral assemblage in our samples. The similar granulometry among the samples suggest that this parameter was not a segregating factor and that the internal dynamics of the lake is determined only by wind action on the surface.

ACKNOWLEDGMENTS

The authors thank the Universidade Federal do Oeste do Pará (UFOPA) for logistical and financial support through the call for proposals 06/2016 PROPPIT/UFOPA-PROFIC; the LabMev at Universidade Federal do Pará (UFPA) for the SEM and cathodoluminescence images of the heavy minerals, and the Mineral Characterization Laboratory at UFPA for the XRD and FTIR analyses. Thanks also to the editor and anonymous reviewers for their suggestions that have been very helpful in improving the manuscript.

REFERENCES

Achab, M.; Cardona, J.P.M.; Gutiérrez-Mas, J.M.; Bellón, A.S.; Gonzalez-Caballero, J.L. 2017. Sedimentary provenance and depositional history of Cadiz Bay (SW Spain) based on the study of heavy minerals surface textures. *Thalassas*, 33: 29-42.

Amigó, J.M.; Bastida, J.; Garcia Agramut, M.J.; Sanz, M.; Galvan, J. 1987. Crystallinity of Lower Cretaceous kaolinites of Teruel. In: Galfin, E; Perez-Rodriguez, J.L; Cornejo, J. (Ed.). *EUROCLAY Conference*, Sevilla, Spain, p.74-75.

ANA. 2011. Agência Nacional de Águas – Plano Estratégico de Recursos Hídricos dos Afluentes da Margem Direita do Rio Amazonas. Brasília, p. 6.10-6.11.

ANA. 2018. Agência Nacional de Águas – Sistema de Informações Hidrológicas. (http://www.snirh.gov.br/hidroweb/). Accessed on 01 Oct 2018.

Andò, S.; Garzanti, E.; Padoan, M.; Limonta, M. 2012. Corrosion of heavy minerals during weathering and diagenesis: A catalog for optical analysis. *Sedimentary Geology*, 280: 165-178.

Araújo, G.S.; Bicalho, K.V.; Tristão, F.A. 2015. Análise de imagens na determinação da forma e textura de areias. *Revista Brasileira de Ciências do Solo*, 39: 94-99.

Azevedo, T.R. 2017. *Caracterização mineralógica do rejeito magnético de caulim da planta Imerys, da mina Ipixuna - Pará*. Master's dissertation, Instituto Tecnológico Vale, Brazil. 68p. (http://www.itv.org/publicacao/caracterizacao-mineralogica-do-rejeito-magnetico-de-caulim-da-planta-imerys-da-mina-ipixuna-para/).

Bhaskar, J.; Saikia, B.J.; Parthasarathy, G. 2010. Fourier transform infrared spectroscopic characterization of kaolinite from Assam and Meghalaya, Northeastern India. *Journal of Modern Physics*, 1: 206-210.

Bertassoli Jr., D.J.; Sawakuchi, A.O.; Sawakuchi, H.O.; Pupim, F.N.; Hartmann, G.;A.; McGlue, M.M.; *et al.* 2017. The fate of carbon in sediments of the Xingu and Tapajós clearwater rivers, Eastern Amazon. *Frontiers in Marine Science,* 22: 1-14.

Bicudo, D.C.; Tremarin, P.I.; Almeida, P.D.; Zorzal-Almeida, S.; Wengrat, S.; Faustino, S.B.; *et al.* 2016. Ecology and distribution of *Aulacoseira* species (Bacillariophyta) in tropical reservoirs from Brazil. *Diatom Research*, 31: 199-215.

Brown, G.E.; Trainor, T.P.; Chaka, A.M. 2008. Geochemistry of mineral surfaces and factors affecting their chemical reactivity. In: Nilsson, A.; Pettersson, L.G.M.; Norskov, J.K. (Eds.). *Chemical Bonding at Surfaces and Interfaces*, Elsevier, Amsterdam, p. 457–509.

Carvalho, N.O. 2008. *Hidrossedimentologia Prática*. CPRM – Companhia de Pesquisa em Recursos Minerais, Rio de Janeiro, 372p.

Chamley, H. 1989. *Clay Sedimentology*. Springer Verlag, Berlin, 623p.

Chukanov, N.V. 2014. *Infrared spectra of mineral species*. Springer, Netherlands, 1726p.

Cohen, J.C.P.; Fitzjarrald, D.R.; D'Oliveira, F.A.F.; Saraiva, I.; Barbosa, I.R.S.; Gandu, A.W.; Kuhn, P.A. 2014. Radar-observed spatial and temporal rainfall variability near the Tapajós-Amazon confluence. *Revista Brasileira de Meteorologia*, 29: 23-30.

Corfu, F.; Hanchar, J.M.; Hoskin, P.W.O.; Kinny, P. 2003. Atlas of zircon textures. *Reviews in Mineralogy and Geochemistry*, 53: 469-500.

Coutinho, M.G.N. 2008. Geologia do Craton Amazônico. In: Coutinho, M.G.N. (Ed.). *Província mineral do Tapajós: geologia, metalogenia e mapa provisional para ouro em SIG*. Serviço Geológico do Brasil, Rio de Janeiro, p.15-34.

Daemon, R.F. 1975. Contribuição a datação da Formação Alter do Chão, Bacia do Amazonas. *Revista Brasileira de Geociências*, 5: 58-84.

Dantas, A.B.; Ribeiro, A.C.S.; Santos, L.O.; Mendes, A.C.; Mendes, K.C. 2017. Characterization and distribution of the background sediments of Green Lake, Alter do Chão village, Pará State. *Proceedings of the II Congresso Internacional de Hidrossedimentologia,* Foz do Iguaçu, Brazil. p.19-24.

Deer, W.A.; Howie, R.A.; Zussman, J. 2013. *An Introduction to the Rock-Forming Minerals.* Mineralogical Society of Great Britain and Ireland, Cambridge, 498p.

Doucet, L.S; Ionov, D.A.; Golovin, A.V. 2013. The origin of coarse garnet peridotites in cratonic lithosphere: new data on xenoliths

from the Udachnaya kimberlite, central Siberia. *Contributions to Mineralogy and Petrology*, 165: 1225–1242.

Frost, R.L. 1998. Hydroxyl deformation in Kaolins. *Clays Clay Mineralogy*, 46: 280-289.

Gagnevin, D.; Daly, J.S.; Kronz, A. 2010. Zircon texture and chemical composition as a guide to magmatic processes and mixing in a granitic environment and coeval volcanic system. *Contributions to Mineralogy and Petrology*, 159: 579–596.

Gualtieri, C.; Iannirubertо. M.; Filizola, N.; Santos, R.; Endreny, T. 2017. Hydraulic complexity at a large river confluence in the Amazon basin. Ecohydrology, 10: e1863.

Guyot, J.L.; Jouanneau, J.M.; Soares, L.; Boaventura, G.R.; Maillet, N.; Lagane, C. 2007. Clay mineral composition of river sediments in the Amazon Basin. *Catena*, 71: 340–356.

Helland, P.E.; Huang, P.; Diffendal, R.F. 1997. SEM Analysis of quartz sand grain surface textures indicates alluvial/colluvial origin of the Quaternary "Glacial" Boulder Clays at Huangshan (Yellow Mountain), East-Central China. *Quaternary Research*, 48: 177-187.

Hubert, J.E. 1962. A zircon-tourmaline-rutile maturity index and the interdependence of the composition of heavy mineral assemblages with the cross composition and texture of sandstones. *Journal of Sedimentary Petrolology*, 32: 440–450.

Irion, G.; Bush, M.B.; Nunes de Mello, J.A.; Stüben, D.; Neumann, T; Müller, G. 2006. A multiproxy palaeoecological record of Holocene lake sediments from the Tapajós River, Eastern Amazonia. *Palaeogeography, Palaeoclimatology, Palaeoecology*, 240: 523-535.

Jesus, L.V.; Andrade, A.C.S.; Silva, M.G; Rodrigues, T.K. 2014. Distribuição espacial das características granulométricas, morfoscópicas e composicionais dos sedimentos das praias de Aracaju, Sergipe. *Scientia Plena*, 10: 1-15.

Krinsley, D.H.; Doornkamp, J.C. 2011. *Atlas of Quartz Sand Surface Textures*. Cambridge University Press, London, 91p.

Krynine, P.D. 1946. The tourmaline group in sediments. *Journal of Geology*, 54: 65-87.

Kurumathoor, R.; Franz, G. 2018. Etch pits on beryl as indicators of dissolution behavior. *European Journal of Mineralogy*, 30: 107-124.

Lackey, J.S.; Romero, G.A.; Bouvier, A-S.; Valley, J.W. 2012. Dynamic growth of garnet in granitic magmas. *Geology*, 40: 171-174.

Landim, P.M.B.; Bósio, N.J.; Wu, F.T.; Castro, P.R.M. 1983. Minerais pesados provenientes do leito do rio Amazonas. *Acta Amazonica*, 13: 51-72.

Latrubesse, E.M.; Stevaux, J.C.; Sinha, R. 2005. Tropical Rivers. *Geomorphology*, 70: 187–206.

Lord, M.L., Germanoski, D., and Allmendinger, N.E. 2009. Fluvial geomorphology: Monitoring stream systems in response to a changing environment. In: Young, R.; Norby, L. (Eds.). *Geological Monitoring*. Geological Society of America, Boulder, p 69–103.

Machado; G.M.V.; Albino, J.; Leal, A.P; Bastos, A.C. 2016. Quartz grain assessment for reconstructing the coastal palaeoenvironment. *Journal of South American Earth Sciences*, 70: 353-367.

Mange, M.A.; Maurer, H.F.W. 2012. *Heavy Minerals in Colour*. Springer Netherlands, Amsterdam, 160p.

Marcinkowski, B.; Mycielska-Dowgiałło, E. 2013. Heavy-mineral analysis in Polish investigations of Quaternary deposits: a review. *Geologos*, 19: 5–23

Medeiros Filho, L.C.; Lafon, J.M.; Souza Filho, P.W.M. 2016. Pb-Sr-Nd isotopic tracing of the influence of the Amazon River on the bottom sediments in the lower Tapajós River. *Journal of South American Earth Sciences*, 70: 36-48.

Mendes, A.C. 2010. *Litofácies e minerais pesados da Formação Alter do Chão (Cretáceo), região de Óbidos-PA, parte central da bacia do Amazonas*. Master's dissertation, Universidade Federal do Pará, Brazil, 56p. (http://bdtd.ibict.br/vufind/Record/UFPA_cac01e65285443b20aa6362a3dacb0d5)

Mendes, A.C. 2015. *Fáceis e proveniência de depósitos siliciclásticas cretáceos e néogenos da Bacia do Amazonas: implicações para a história evolutiva do Proto-Amazonas*. Doctoral thesis, Universidade Federal do Pará, Brazil, 116p.

Mendes, A.C.; Santos Júnior, A.E.A.; Nogueira, A.C.R. 2013. Petrografia de arenitos e minerais pesados da Formação Alter do Chão, bacia do Amazonas. *Proceedings of the 13º Simpósio de Geologia da Amazônia*, Belém. p.22-26.

Mendes, A.C.; Truckenbrod, W.; Nogueira, A.C.R. 2012. Análise faciológica da Formação Alter do Chão (Cretáceo, Bacia do Amazonas), próximo à cidade de Óbidos, Pará, Brasil. *Revista Brasileira de Geociências*, 42: 39-57.

Moore, D.M.; Reynolds Jr., R.C. 1997. *X-Ray Diffraction and the Identification and Analysis of Clay Minerals*. Oxford University Press, New York, 378p.

Moquet, J.S.; Guyot, J.L.; Crave, A.; Viers, J.; Filizola, N.; Martinez, J-L. *et al*. 2016. Amazon River dissolved load: temporal dynamics and annual budget from the Andes to the ocean. *Environmental Science and Pollution Research*, 23: 11405–11429.

Moral Cardona, J.P.; Gutiérrez Mas, J.M.; Sánchez Bellón, A.; Domínguez-Bella, S.; Martínez López, J. 2005. Surface textures of heavy-mineral grains: a new contribution to provenance studies. *Sedimentary Geology*, 174: 223–235.

Morton, A.C. 1985. A new approach to provenance studies: electron microprobe analysis of detrital garnets from Middle Jurassic sandstones of the northern North Sea. *Sedimentology*, 32: 553-566.

Morton, A.C.; Hallsworth, C. 1994. Identifying provenience-specific features of detrital heavy mineral assemblages in sandstones. *Sedimentary Geology*, 90: 241-256.

Morton, A.C.; Hallsworth, C. 1999. Processes controlling the composition of heavy mineral assemblages in sandstones. *Sedimentary Geology*, 124: 3-29.

Nascimento Jr., D.R.; Sawakuchi, A.O.; Guedes, C.C.F.; Giannini, P.C.F.; Grohmann, C.H.; Ferreira, M.P. 2015. Provenance of sands from the confluence of the Amazon and Madeira rivers based on detrital heavy minerals and luminescence of quartz and feldspar. *Sedimentary Geology,* 316: 1–12.

Nascimento, D.A.; Garcia, M.G.L.; Mauro, C. A. 1976. *Projeto Radam - Brasil. Folha SA.21–Santarém: geologia, geomorfologia,*

pedologia, vegetação e uso potencial da terra. *v. 10*. Departamento Nacional de Produção Mineral, Rio de Janeiro, p.132-181.

Nevado, J.J.B.; Martín-Doimeadios, R.C.R.; Bernardo, F.J.G.; Moreno, M.J.; Herculano, A.M.; Nascimento, J.L.M.; Crespo-López, M.E. 2010. Mercury in the Tapajós River basin, Brazilian Amazon: A review. *Environment International,* 36: 593-608.

Park, E.; Latrubesse, E.M. 2015. Surface water types and sediment distribution patterns at the confluence of mega rivers: The Solimões-Amazon and Negro Rivers junction. *Water Resources Research*, 51: 6197-6213.

Pettijohn, F.J.; Potter, P.E; Siever, R. 1987. *Sand and Sandstones*. 2nd ed. Springer-Verlag, New York, 533p.

Rajganapathi, V.C.; Jitheshkumar, C.; Sundararajan, M.; Bhat, K.H.; Velusamy, S. 2013. Grain size analysis and characterization of sedimentary environment along Thiruchendur coast, Tamilnadu, India. *Arabian Journal of Geosciences*, 6: 4717-4728.

Rocha, J.F.G. 2014. *Solos da região sudeste do município de Santarém, estado do Pará: mapeamento e classificação*. Master's dissertation, Universidade Federal do Oeste do Pará, Brazil. 61p. (http://www2.ufopa.edu.br/ufopa/academico/pos-graduacao/banco-de-teses/ppg-rna/turma-de-2012/rocha-josan-flavio-goncalves-da/at_download/file).

Rossetti, D.F. 2014. Imaging underwater neotectonic structures in the Amazonian lowland. *The Holocene,* 24: 1269–1277.

Saikia, B.J.; Parthasarathy, G. 2010. Fourier Transform Infrared Spectroscopic Characterization of Kaolinite from Assam and Meghalaya, Northeastern India. *Journal of Modern Physics*, 1: 206-210.

Sawakuchi, A.O.; Jain, M.; Mineli, T.D.; Nogueira, L.; Bertassoli, D.J.; Häggi, C. *et al*. 2018. Luminescence of quartz and feldspar fingerprints provenance and correlates with the source area denudation in the Amazon River basin. *Earth and Planetary Science Letters*, 492: 152–162.

Shahbazi, H.; Salami, S.; Siebel, W. 2014. Genetic classification of magmatic rocks from the Alvand plutonic complex, Hamedan, western Iran, based on zircon crystal morphology. *Geochemistry*, 74: 577-584

Shoval, S.; Yariv, S.; Michaelian, K.H.; Lapides, I.; Boudeuille, M.; Panczers, G. 1999. *Colloid Interface Science*, 212: 523.

Sioli, H. 2011. *The Amazon: Limnology and Landscape Ecology of a Mighty Tropical River and its Basin*. Springer, London, 800p.

Sorribas, M.V.; Paiva, R.C.D.; Melack, J.M.; Bravo, J.M.; Jones, C.; Carvalho, L.; Beighley, E.; Forsberg, B. Costa, M.H. 2016. Projections of climate change effects on discharge and inundation in the Amazon basin. *Climatic Change,* 136: 555-570.

Sousa, D.R.; Cabral, A.S.; Nobre, D.; Lobato, H.; Goch, Y.G.F.; Peleja, J.R.P.; *et al*. 2009. Diagnóstico sedimentar e físico-químico dos igarapés no trecho de Santarém a vila balneária de Alter do Chão-PA. *Em Foco*, 11: 75-85.

Souza-Filho, P.W.; Guimarães, J.T.F.; Silva, M.; Costa, F.R.; Sahoo, P.K.; Maurity, C.; *et al*. 2016. Basin morphology, sedimentology and seismic stratigraphy of an upland lake from Serra dos Carajás, southeastern Amazon, Brazil. *Boletim do Museu Paraense Emílio Goeldi. Ciências Naturais*, 11: 71-83.

Sturm, R. 2010. Morphology and growth trends of accessory zircons from various granitoids of the South-western Bohemian Massif (Moldanubicum, Austria). *Geochemistry*, 70: 185-196

Suresh, N.K.; Sumit, S.; Ghosh, K.; Sangode, S.J. 2004. Clay-mineral distribution patterns in late Neogene fluvial sediments of the Subathu sub-basin, central sector of Himalayan foreland basin: implications for provenance and climate. *Sedimentary Geology*, 163: 265-278.

Tortosa, A.; Palomares, M.; Arribas, J. 1991. Quartz grain types in Holocene deposits from the Spanish Central System: some problems in provenance analysis. In: Morton, A.C.; Todd, S.P.; Haughton, P.D.W. (Ed.). *Developments in Sedimentary Provenance Studies*. Geological Society of London, Special Publication 57, p.47– 54.

Viers, J.; Roddaz, M.; Filizola, N.; Guyot, J.L.; Sondag, F.; Brunet, P.; *et al*. 2008. Seasonal and provenance controls on Nd–Sr isotopic compositions of Amazon rivers suspended sediments and implications for Nd and Sr fluxes exported to the Atlantic Ocean. *Earth and Planetary Science Letters*, 274: 511–523.

Wampler, P.J. 2012. Rivers and Streams - Water and Sediment in Motion. *Nature Education Knowledge*, 3: 18-21.

Wittmann, H.; von Blanckenburg, F.; Maurice, L.; Guyot, L.; Filizola, N.; Kubik, P.W. 2010. Sediment production and delivery in the Amazon River basin quantified by in situ-produced cosmogenic nuclides and recent river loads. *Geological Society of America* B*ulletin,* 123: 934-950.

Woronko, B.; Pisarska-Jamroży, M.; van Loon, A.J. 2015. Reconstruction of sediment provenance and transport processes from the surface textures of quartz grains from Late Pleistocene sandurs and an ice-marginal valley in NW Poland. *Geologos*, 21: 105–115.

Zhu, X.; Zhu, Z.; Lei, X.; Yan, X. 2016. Defects in structure as the sources of the surface charges of kaolinite. *Applied Clay Science*, 124-125: 127-136.

Zuther, M.; Brockamp, O.; Clauer, N. 2000. Composition and origin of clay minerals in Holocene sediments from the South- Eastern North Sea. *Sedimentology*, 47: 119-134.

RECEIVED: 31/01/2019
ACCEPTED: 30/12/2019
ASSOCIATE EDITOR: José Stevaux